Microphase-Separated Block Copolymers Comprising Low Surface Energy Fluorinated Blocks and Hydrophilic Blocks: Synthesis and Characterization

Michelle E. Arnold,[†,‡] Kazukiyo Nagai,[†,‡] Richard J. Spontak,[‡] Benny D. Freeman,[*,§] Denis Leroux,[†,||,#] Douglas E. Betts,[†,||] Joseph M. DeSimone,[*,||] Francis A. DiGiano,[#] Camille K. Stebbins,[†,||] and Richard W. Linton[†,||]

Department of Chemical Engineering, North Carolina State University, Raleigh, North Carolina 27695-7905; Department of Chemical Engineering, University of Texas at Austin, Austin, Texas 78758-4445; and Department of Chemistry and Department of Environmental Sciences and Engineering, University of North Carolina at Chapel Hill, Chapel Hill, North Carolina 27599-7400

Received November 12, 2001; Revised Manuscript Received December 27, 2001

ABSTRACT: The synthesis and characterization of diblock and triblock copolymers produced by a two-component iniferter system is reported. These materials, designed for possible water treatment applications, consist of a hydrophilic poly(2-dimethylaminoethyl methacrylate) (PDMAEMA) block and a very low surface energy poly(1,1′-dihydroperfluorooctyl methacrylate) (PFOMA) or poly(1,1,2,2-tetrahydroperfluorooctyl acrylate) (PTAN) block. Angle-dependent X-ray spectroscopy results and water contact angle measurements indicate that the surfaces of PDMAEMA-*b*-PFOMA diblock copolymers consist primarily of PFOMA. Transmission electron microscopy reveals that the block copolymers are microphase-separated, exhibiting either cylindrical or layered morphologies that do not change appreciably upon exposure to water. Both water uptake and water flux increase with increasing PDMAEMA content.

Introduction

Requirements for membranes designed for drinking water and wastewater treatment include adequate permeability and solute rejection.[1,2] Polymeric membranes would be used much more extensively for this purpose if lower fouling materials were available.[1,3,4] In this regard, Hamza et al.[5] modified the surfaces of porous poly(ether sulfone) ultrafiltration membranes with fluorotelomers and found that these modified membranes were less susceptible to fouling by oil/water mixtures than unmodified ones. The modified membranes were also more permeable to oil/water emulsions than their unmodified analogues.

Block copolymers offer an additional degree of freedom in tailoring polymer properties[6,7] and can, in many cases, be synthesized in a convenient and well-controlled manner using the iniferter controlled free-radical polymerization technique developed by Otsu and coworkers.[8−11] However, only a limited number of studies have evaluated block copolymers as possible membrane materials for water treatment applications.[12−18] The present work describes the iniferter synthesis and characterization of a novel series of microphase-separated block copolymers, consisting of a poly(2-dimethylaminoethyl methacrylate) (PDMAEMA) block and one or two fluorocarbon blocks composed of either poly(1,1′-dihydroperfluorooctyl methacrylate) (PFOMA) or poly(1,1,2,2-tetrahydroperfluorooctyl acrylate) (PTAN). The PDMAEMA block is hydrophilic and, therefore, facilitates water transport through these materials, while the PFOMA or PTAN blocks have low surface energies and could potentially increase fouling resistance. The surface and bulk morphological characteristics of these materials are investigated by angle-dependent X-ray spectroscopy (ADXPS), static contact angle measurements, and transmission electron microscopy (TEM). In addition, water uptake and water flux values are reported.

Experimental Section

Materials. The monomers 2-(dimethylaminoethyl methacrylate) (DMAEMA) and 1,1′-dihydroperfluorooctyl methacrylate (FOMA) were obtained from Aldrich Chemical Co. (Milwaukee, WI) and 3M Co. (Minneapolis, MN), respectively. They were passed through an alumina column to remove inhibitor and deoxygenated in an argon purge prior to use. Some DMAEMA monomer was also purified by vacuum distillation at 55 °C. The monomer 1,1,2,2-tetrahydroperfluorooctyl acrylate (TAN) was graciously provided by E. I. duPont de Nemours & Co. (Wilmington, DE) and was purified by passage through an alumina column that was heated by a water jacket to melt the TAN. Tetraethylthiuram disulfide (TD) was obtained from Aldrich and recrystallized twice from methanol prior to use. Proton nuclear magnetic resonance (^{1}H NMR) was used to verify TD purity. The iniferters benzyl *N*,*N*-diethyldithiocarbamate (BDC) and xylylene bis(*N*,*N*-diethyl dithiocarbamate) (XDC) were synthesized as described in the literature.[8,9,19] Methanol, tetrahydrofuran (THF), hexanes, and acetone were obtained from Mallinckrodt, Inc. (St. Louis, MO) and were used as received. Casting solvents—1,1,2-trichlorotrifluoroethane (F-113) and α,α,α-trifluorotoluene (TFT)—were obtained at 99+% purity from DuPont and Aldrich, respectively, and were used without further purification. Industrial grade compressed air was obtained from National Specialty Gases (Raleigh, NC) and was used as received. Ultrapure water used in this study was produced using a water purifica-

* To whom correspondence should be addressed.
† Present addresses: M.E.A., Novozymes North America, Inc., Franklinton, NC 27525; K.N., CSIRO Molecular Science, Private Bag 10, Clayton South, VIC 3169, Australia; D.L, SiPix Imaging, Milpitas, CA 95035; D.E.B., ONDEO-Nalco, Naperville, IL 60563; C.K.S., MeadWestvaco, Charleston, SC 29423; R.W.L., Department of Chemistry, University of Oregon, Eugene, OR 97403.
‡ North Carolina State University.
§ University of Texas at Austin.
|| Department of Chemistry, University of North Carolina at Chapel Hill.
Department of Environmental Sciences and Engineering, University of North Carolina at Chapel Hill.

10.1021/ma0119631 CCC: $22.00 © 2002 American Chemical Society
Published on Web 03/27/2002

tion system manufactured by Millipore Corporation (Bedford, MA). This system consisted of two prefilters (5 μm and carbon) followed by a Rios 16 reverse osmosis unit and a Milli-Q Plus TOC ultrapure water purification system in series.

Synthesis of Telechelic PDMAEMA. Telechelic monofunctional PDMAEMA (PDMAEMA-BDC) was synthesized by free-radical polymerization using monofunctional BDC as the iniferter. Bulk polymerizations conducted in quartz flasks equipped with stir bars were typically performed to between 70 and 80% conversion. A typical polymerization is described here: 0.1875 g of BDC and 0.7 mg of TD were dissolved in 30 g of deinhibited DMAEMA. The flask was subsequently sealed with a septum and purged with argon. The solution was photolyzed for 1 h in a 16-bulb Rayonet photoreactor equipped with 350 nm bulbs. Afterward, the reaction medium was diluted with THF, and the polymer was collected by precipitation into hexanes and dried under vacuum. The yield was determined gravimetrically. Telechelic bifunctional PDMAEMA (PDMAEMA-XDC) was synthesized in analogous manner using a two-component XDC/TD iniferter system rather than the BDC/TD system used to prepare PDMAEMA-BDC. In both polymerizations, the TD does not initiate DMAEMA polymerization but instead helps to control the polymerization by supplying an excess of the end-capping dithiocarbamate radicals.[20]

Block Copolymer Synthesis. Diblock copolymers were synthesized by the subsequent photopolymerization of FOMA monomer using previously synthesized telechelic monofunctional PDMAEMA-BDC as the macroiniferter. In a typical solution for polymerization, 5 g of PDMAEMA-BDC was dissolved in TFT and 19.4 g of deinhibited FOMA was added to the quartz reaction flask. The molar ratio of FOMA monomer to PDMAEMA-BDC iniferter was 238. The reaction vessel was sealed with a septum, purged with argon, and then photolyzed for 27 h in the same reactor described above. The resulting polymer was collected by precipitation in an excess of hexanes and dried under vacuum at 60 °C for 16 h. The block copolymer was purified by Soxhlet extraction using methanol for 15 h to remove residual PDMAEMA homopolymer. The resulting copolymer was characterized by ^{1}H NMR in a mixed solvent of F-113 and d_6-acetone. Triblock copolymers were synthesized and purified in similar fashion by the subsequent photopolymerization of FOMA or TAN monomer using previously prepared PDMAEMA-XDC as the macroiniferter.

Polymer Characterization. The UV spectra were acquired with a Perkin-Elmer Lambda 6 UV−vis spectrophotometer. Molecular weights were estimated by assuming a functionality of one for the polymers synthesized using BDC and a functionality of two for the polymers synthesized using XDC. Composition analysis of the block copolymers was conducted by ^{1}H NMR using a Bruker WM 250 spectrometer. These measurements were performed in a mixed solvent of F-113 and d_6-acetone. Glass transition temperatures were characterized by differential scanning calorimetry (DSC) performed on a Perkin-Elmer DSC-7 calorimeter operated at a heating rate of 10 °C/min in a N_2 atmosphere.

Surface Composition Characterization. Films for angle-dependent X-ray photoelectron spectroscopy (ADXPS) were spun-cast at either 500 or 1000 rpm from 1% (w/v) solutions in F-113 onto precleaned silicon substrates. Block copolymer films were annealed at 100 °C for 24 h in covered petri dishes in an air atmosphere to promote equilibration. Samples exposed to water were first annealed, soaked in deionized water for 4 h, and then vacuum-dried before examination by ADXPS.

A Physical Electronics (PHI) model 5400 spectrometer equipped with a hemispheric capacitor analyzer was used to perform the ADXPS measurements. X-rays from a monochromatic Al K$\alpha_{1,2}$ source irradiated a 1 mm diameter spot size on the samples. The binding energy scale of the instrument was calibrated by setting $Au_{4f7/2}$, $Cu_{1p3/2}$, and $Ag_{3d5/2}$ to 84.0, 932.6, and 368.3 eV, respectively. Typical operating conditions for the analyses were as follows: 2×10^{-8} Torr chamber pressure; 15 kV; 500−600 W; 35−40 mA for the Al X-ray source. Elemental survey scans from 0 to 1000 eV were acquired with a pass energy of 89.5 eV, while high-resolution scans of the C_{1s}, F_{1s} and O_{1s} regions were acquired with pass energies of 17.9 or 35.8 eV. To minimize beam-induced damage, electron flooding was not used to compensate for charging. Data were acquired at takeoff angles of 20, 40 and 70° between the sample and analyzer. On the basis of an estimated[21] inelastic mean free path for a C_{1s} photoelectron of 27 Å originating from organic materials, these angles correspond to approximate sampling depths of 2.8, 5.2, and 7.6 nm, respectively. The ADXPS signal at a given sampling depth corresponds to a convolution of measurements from all components down to that depth, with an exponential attenuation of photoelectrons from subsurface layers due to scattering.[22] The C, O, F, and N (when applicable) atomic percentages were determined after including the appropriate instrumental sensitivity factors. An in-depth convolution analysis of the spectra was performed using a least-squares curve-fitting algorithm. Peak positions were determined according to previously established binding energies and were thus held relatively constant. The peak parameters that were allowed to vary included the peak height, full width at half-maximum (fwhm), and percentage Gaussian. The program decomposed both the C_{1s} and O_{1s} spectra into the various chemical components corresponding to the functional groups comprising the polymer. Spectra were then charge-corrected to align the hydrocarbon component of the C_{1s} region to 285.0 eV.

Contact Angle Measurements. Films for static contact angle measurements were spun-cast at either 500 or 1000 rpm from 1% (w/v) solutions in F-113 onto aluminum substrates. Water contact angles were measured by the pendant drop technique using a Rame-Hart model 100-00 goniometer.

Morphological Characterization. Electron-transparent specimens for transmission electron microscopy (TEM) were prepared by casting 200−250 μm films from filtered 12.5−25% (w/v) solutions in Teflon molds, followed by slow solvent evaporation. The PDMAEMA-*b*-PFOMA and PFOMA-*b*-PDMAEMA-*b*-PFOMA block copolymers were dissolved in F-113; the solvent for PTAN-*b*-PDMAEMA-*b*-PTAN was TFT. To assess whether morphological rearrangement occurs in the presence of water, half of each specimen was exposed to water, while the other half was left unexposed to water. The water-exposed samples were immersed in ultrapure water for 6 h and then dried in a vacuum oven at ambient temperature for 1 h to avoid microtoming difficulties. Bulk films were subsequently sectioned using a Reichert-Jung Ultracut-S cryoultramicrotome operated at −100 °C. The resultant thin sections were exposed to the vapor of 2% RuO_4(aq) for 7 min to stain the PDMAEMA-rich microdomains. Transmission electron micrographs were obtained using a Zeiss EM902 electron spectroscopic microscope operated at 80 kV and energy-loss settings (ΔE) of up to 100 eV. Microdomain thicknesses were discerned from direct measurement of the images. Each value represents the average of a minimum of 60 measurements collected from multiple negatives of the same specimen.

Water Uptake and Flux Measurements. Dense films with uniform thicknesses of 40−180 μm were cast from 5 to 10% (w/v) polymer solutions onto Teflon plates at ambient temperature. The solvents for the PFOMA- and PTAN-based copolymers were F-113 and TFT, respectively. Water uptake measurements were conducted as described elsewhere.[17] Average values of water uptake are reported for each copolymer composition. Water flux was determined at ambient temperature using an Advantec Microfiltration Systems (Pleasanton, CA) model UHP-40 dead-end filtration cell with a membrane area of 11.5 cm^2. For block copolymer formulations available in limited quantities, smaller films were cast and mounted between two pieces of aluminum tape prior to loading in the stirred cell. A compressed air cylinder was used to maintain upstream pressures at 10−50 psig, while the downstream pressure was kept at atmospheric pressure. Water flux values

Scheme 1

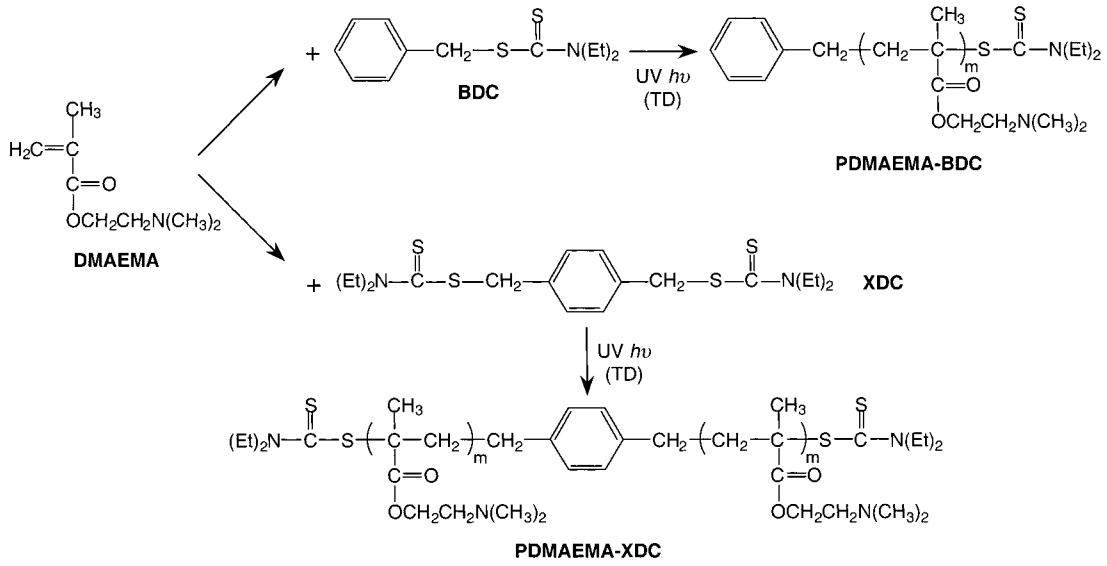

Table 1. Synthesis of Telechelic PDMAEMA Using BDC or XDC as the Iniferter

sample	iniferter[a]	DMAEMA/iniferter molar ratio	polymerization time (h)	DMAEMA conversion (%)[b]	$\bar{M}_n \times 10^{-3}$
1	BDC	244	1.0	75	29[c]
2	BDC	225	2.0	77	27[c]
3	BDC	573	1.6	35	32[c]
4	XDC	1041	2.0	68.5	46[d]

[a] The assumed values of f for BDC and XDC are 1 and 2, respectively. [b] Determined by ^{1}H NMR. [c] Estimated from the conversion of the DMAEMA monomer and eq 2 on the assumption of a perfect living polymerization. [d] Determined by UV spectroscopy.[23]

were determined from

$$\text{water flux} = \left(\frac{1}{A}\right)\frac{dV}{dt} \tag{1}$$

where dV/dt is the volumetric flow rate of permeate collected within a graduated cylinder (L/h) and A is the membrane area (m^2).

Results and Discussion

Synthesis and Characterization of Telechelic PDMAEMA. Monofunctional and bifunctional telechelic PDMAEMA samples have been synthesized by the iniferter technique using BDC and XDC, respectively (Scheme 1). Polymerization conditions and characteristics for the synthesized macroiniferters are summarized in Table 1. Since DMAEMA polymerizes easily, a small amount of TD is used as a chain transfer agent in each polymerization. The added TD supplies a slight excess of dithiocarbamate radicals which help to control the reactions.[20,23] In a separate experiment, we have tried to polymerize DMAEMA using only TD as the initiator. However, the polymerization rate is very slow (13% yield after 40 h at 60 °C). Since no dithiocarbamate end groups are detected by ^{1}H NMR, we conclude that TD does not initiate the polymerization of DMAEMA. It follows, then, that TD acts as a reversible end-capping agent.

The conversion values in Table 1 have been determined by ^{1}H NMR from the ratio of the peak areas associated with the CH_2=C− protons in the DMAEMA monomer and the −CH_2−C− protons in the telechelic PDMAEMA backbone. Generally speaking, these polymerizations are relatively rapid. With the exception of sample 3, ca. 70−80% DMAEMA conversion is attained within 1−2 h. Determination of the molecular weight of a PDMAEMA macroiniferter is, however, problematic. All attempts to characterize the number-average molecular weight, $\bar{M}_n$, of each macroiniferter by gel permeation chromatography (GPC) have been unsuccessful. The values of $\bar{M}_n$ provided in Table 1 for the monofunctional, telechelic PDMAEMA-BDC are estimated by assuming a perfect living polymerization in which all polymer chains initiate simultaneously. Moreover, the chains are presumed to propagate at the same time without any termination reactions. In this idealized scenario, $\bar{M}_n$ of telechelic PDMAEMA can be estimated from

$$\bar{M}_n = C\frac{[M]_0}{[I]}M_{monomer} \tag{2}$$

where C is the conversion determined from ^{1}H NMR, $[M]_0$ is the initial number of moles of DMAEMA monomer, [I] is the number of moles of initiator (BDC or XDC) in the system (assumed to react to completion), and $M_{monomer}$ is the molecular weight of the DMAEMA monomer. Clearly, this approach is only rigorous in describing the synthesis of monodisperse polymer chains of uniform length, which is not strictly true for the polymerizations performed here.

A crude estimate of $\bar{M}_n$ for the bifunctional, telechelic PDMAEMA-XDC is deduced from UV spectroscopy using[23]

$$\bar{M}_n = \frac{C_{polymer}}{fC_{end}} \tag{3}$$

where $C_{polymer}$ is the concentration (g/L) obtained by dissolving a known mass of polymer in a volumetric quantity of solvent, and f is the functionality which is

Table 2. Synthesis and Molecular Characteristics of Diblock and Triblock Copolymers Derived from PDMAEMA

run	$\bar{M}_n \times 10^{-3}$ telechelic PDMAEMA	fluorocarbon monomer	fluorocarbon/telechelic PDMAEMA molar ratio charged to the reactor	block copolymer conversion (%)	$\bar{M}_n \times 10^{-3}$ block copolymer[a]	$\bar{M}_n \times 10^{-3}$ fluorocarbon block[a]	PDMAEMA (mol %)
			PDMAEMA-BDC				
1	44	FOMA	2483	38	791	747	15
2	29[b]	FOMA	238	52	111	82	52
3	27[b]	FOMA	226	40	94	67	55
4	27[b]	FOMA	177	38	78	51	61
5	32[b]	FOMA	224	28	79	47	67
6	29[b]	FOMA	123	58	69	40	69
			PDMAEMA-XDC				
7	46[c]	TAN	ca. 138	64	110	64 (32 each block)	69
8	46[c]	FOMA	314	66	144	98 (49 each block)	59

[a] Molecular weights are determined from ^{1}H NMR and $\bar{M}_n$ of the PDMAEMA prepolymer. [b] Estimated from the conversion of the DMAEMA monomer and eq 2 on the assumption of a perfect living polymerization. [c] Determined by UV spectroscopy.[23]

Scheme 2

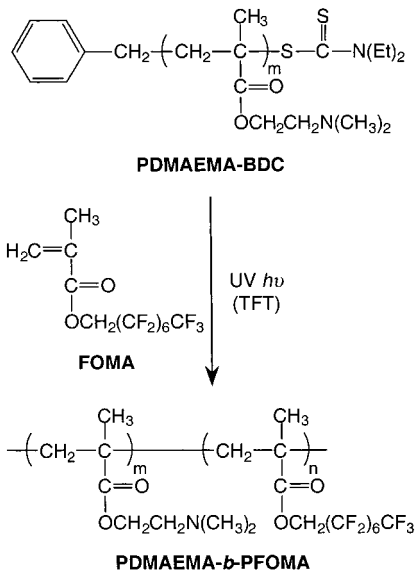

set equal to 2 (on the assumption that the polymer will have the same number of end groups as the initiator, XDC). The molar concentration (mol/L) of the *N*,*N*-diethyldithiocarbamate end groups, C_{end} is calculated from Beer's law:

$$C_{end} = \frac{A_{282}}{\epsilon_{282} b} \quad (4)$$

In eq 4, b denotes the cell path length, and A_{282} and ϵ_{282} represent the absorbance and molar absorptivity of the *N*,*N*-diethyldithiocarbamate end group at 282 nm, respectively.[23] Values of A_{282} are obtained directly from the UV spectrum, while ϵ_{282} is determined from the literature[8,19] to be 1.05×10^4 L/(mol/cm). The molecular weights for PDMAEMA-XDC reported in Tables 1 and 2 correspond to averages from calculations performed for three different polymer concentrations. Individual values of $\bar{M}_n$ are typically within 10% of these average values.

Synthesis and Characterization of Block Copolymers. Diblock and triblock copolymers have been synthesized by the subsequent polymerization of FOMA or TAN monomer by monofunctional PDMAEMA-BDC (Scheme 2) and bifunctional PDMAEMA-XDC (Scheme 3), respectively. Data from these polymerizations are summarized in Table 2. Conversion of the fluorinated monomers ranges from ca. 30 to 65%. The block copolymers have been purified by Soxhlet extraction with methanol to remove unreacted telechelic PDMAEMA. Unreacted fluorocarbon monomer is essentially removed during precipitation in hexanes before extraction. The compositions of the block copolymers have been subsequently characterized by ^{1}H NMR. Figure 1 displays a representative ^{1}H NMR spectrum for a PTAN-*b*-PDMAEMA-*b*-PTAN copolymer.[23] The resonance at 4.4 ppm is attributed to the methylene protons in the PDMAEMA side chain that are closest to the ester linkage: $OCH_2CH_2N(CH_3)_2$. The resonance at 4.1 ppm identifies the methylene protons in the PTAN side chain: $OCH_2(CF_2)_{6-10}CF_3$. The PDMAEMA content (mol %) of the block copolymers is determined directly from the ratio of the areas under these two peaks.

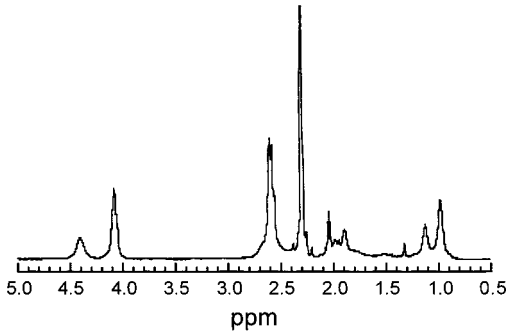

Figure 1. Representative ^{1}H NMR spectrum of a PTAN-*b*-PDMAEMA-*b*-PTAN triblock copolymer.

Values of $\bar{M}_n$ corresponding to the fluorinated blocks are calculated from the estimated molar masses of the PDMAEMA macroiniferters and the ratio of the ^{1}H NMR peak areas described above. In contrast, the $\bar{M}_n$ of each PDMAEMA block is assumed to be equal to the $\bar{M}_n$ of the PDMAEMA prepolymer. Hence, the overall values of $\bar{M}_n$ listed in Table 2 represent the sum of the estimated $\bar{M}_n$ values of the telechelic PDMAEMA and the fluorinated block(s) calculated from ^{1}H NMR data. As mentioned previously, this method for estimating $\bar{M}_n$ is based on the presumption of a perfect, living polymerization. However, the fact that 5−20% telechelic PDMAEMA is removed by extraction after each polymerization clearly indicates that these polymerizations cannot be strictly described as perfect, living systems. Presumably, not all of the telechelic PDMAEMA chains initiate FOMA or TAN polymerization. Nevertheless, the values of $\bar{M}_n$ in Tables 1 and 2 are reasonable estimates that are used hereafter.

Surface Characterization. Angle-dependent X-ray spectroscopy (ADXPS) has been employed to ascertain the chemical composition of unannealed, annealed and

Scheme 3

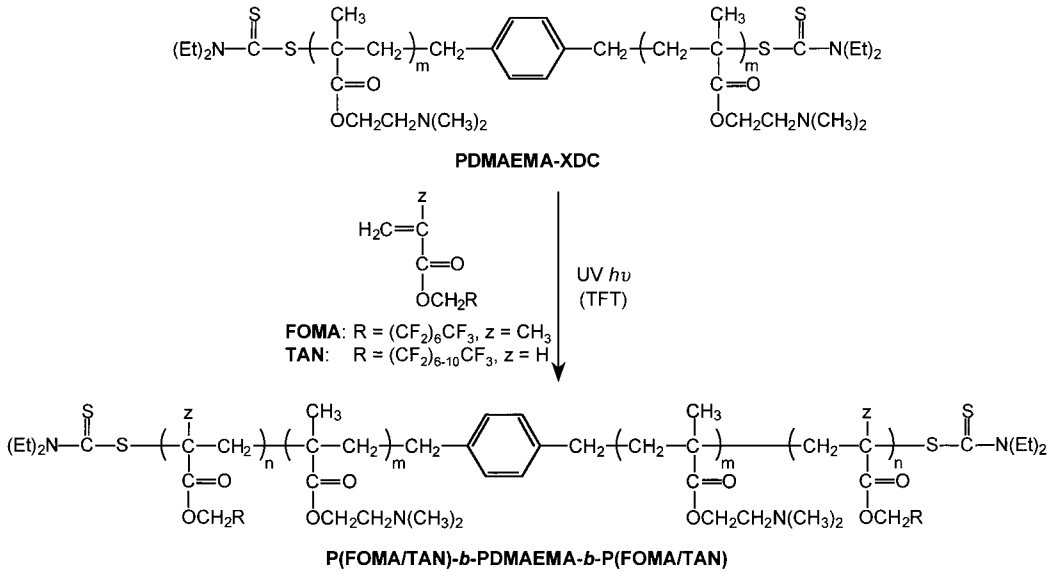

Table 3. Binding Energies of PFOMA, PDMAEMA and PDMAEMA-*b*-PFOMA Copolymers[26]

		binding energies (eV)		
atom	functional group	PFOMA	PDMAEMA[a]	PDMAEMA-*b*-PFOMA
C_{1s}	$-CF_3$	293.8 ± 0.1		293.9 ± 0.01
	$-CF_2$	291.6 ± 0.1		291.6 ± 0.03
	$-C{=}O$	289.4 ± 0.1	289.0	289.5 ± 0.1
	$-CF_2-CH_2-O-C{=}O$	287.6 ± 0.1		287.8 ± 0.1
	$-CH_2-CH_2-O-C{=}O$		286.8	286.9 ± 0.1
	$C-C{=}O$ (PFOMA, PDMAEMA) and $C-N$ (PDMAEMA)	285.8 ± 0.03	285.7	285.8 ± 0.02
	hydrocarbon	285.0	285.0	285.0
F_{1s}		689.5 ± 0.1		689.3 ± 0.2
O_{1s}	$-C-O$	534.3 ± 0.1	533.8	534.0 ± 0.2
	$-C{=}O$	532.7 ± 0.1	532.3	532.6 ± 0.1
N_{1s}			399.1	399.0 ± 0.4

[a] Values are based on reported[25] binding energies of similar polymers.

water-exposed PDMAEMA-*b*-PFOMA diblock copolymer surfaces. The first step required to analyze the surface properties is the structural characterization of the XPS spectra of PFOMA, PDMAEMA, and PDMAEMA-*b*-PFOMA copolymers. The binding energies of the C_{1s}, F_{1s}, O_{1s}, and N_{1s} regions of the polymers are provided in Table 3. Values for PFOMA have been established previously,[24] while those corresponding to PDMAEMA are assigned on the basis of literature values for chemically similar polymers.[25,26] The F_{1s} and O_{1s} windows for the PDMAEMA-*b*-PFOMA copolymers are qualitatively the same as those of PFOMA and PTAN.[24] In analogous manner, the N_{1s} window for these block copolymers is expected to be similar to that of PDMAEMA. The C_{1s} region for the PDMAEMA-*b*-PFOMA copolymers is evaluated by first assigning the C_{1s} components of PFOMA. The C_{1s} binding energies for PDMAEMA listed in Table 3 indicate that all the carbon peaks except for the one corresponding to the $-C-O-C{=}O$ group should closely overlap those of PFOMA. Thus, the C_{1s} spectra can be fit with seven components to account for this functional group. A representative C_{1s} spectrum for the PDMAEMA-*b*-PFOMA copolymer with 69 mol % PDMAEMA is shown in Figure 2.

The ratio of the sum of the $-CF_3$ and $-CF_2$ peak areas to the total area associated with atomic carbon peaks is used to quantify the surface segregation of the fluorinated components. These values are provided in

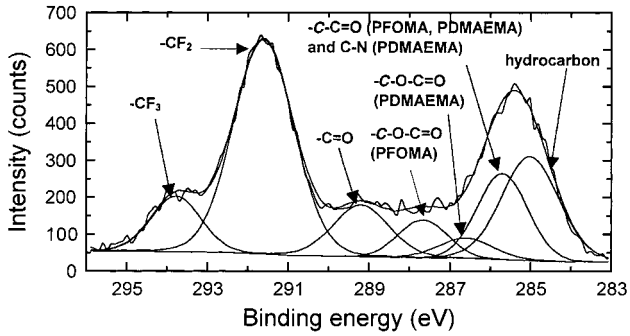

Figure 2. Raw and curve-fit data of C_{1s} spectrum of a PDMAEMA-*b*-PFOMA copolymer with 69 mol % PDMAEMA (PDMAEMA/PFOMA = 2.2) with carbon components assigned.

Table 4 as a function of angle and film conditioning for the PDMAEMA-*b*-PFOMA copolymers, as well as for PFOMA. At all angles, these ratios for the unannealed PDMAEMA-*b*-PFOMA samples are quite similar to each other, despite the fact that the PDMAEMA/PFOMA molar ratios differ by a factor of 2. These values are only 10−15% less than those of unannealed PFOMA homopolymer, suggesting that the block copolymer surfaces consist predominantly, but not entirely, of PFOMA. This result is not surprising since PFOMA has an extremely low surface energy (<11 dyn/cm)[27,28] and is expected to segregate to the polymer−air interface.

Differential scanning calorimetry of the PDMAEMA-*b*-PFOMA copolymer with 69 mol % PDMAEMA reveals

Table 4. The (CF_3 + CF_2)/(Total Carbon) Ratio for PFOMA and PDMAEMA-*b*-PFOMA Copolymers[25,26]

	angle (deg)			
sample	20	40	70	theor
PFOMA				1.41
unannealed	1.73 ± 0.01	1.55 ± 0.01	1.46 ± 0.02	
PDMAEMA(69 mol %)-*b*-PFOMA[a]				0.51
unannealed	1.60 ± 0.01	1.36 ± 0.01	1.22 ± 0.01	
annealed[b]	1.62 ± 0.02	1.50 ± 0.1	1.40 ± 0.002	
water-exposed[c]	1.63 ± 0.01	1.38 ± 0.01	1.48 ± 0.03	
PDMAEMA(52 mol %)-*b*-PFOMA[d]				0.73
unannealed	1.59 ± 0.01	1.31 ± 0.01	1.27 ± 0.01	
annealed[b]	1.71 ± 0.01	1.50 ± 0.004	1.43 ± 0.02	
water-exposed[c]	1.62 ± 0.02	1.45 ± 0.02	1.40 ± 0.02	

[a] PDMAEMA/PFOMA molar ratio = 2.2. [b] Annealed at 100 °C for 24 h in an air atmosphere. [c] Annealed at 100 °C for 24 h in an air atmosphere, soaked for 4 h in deionized water, and vacuum-dried. [d] PDMAEMA/PFOMA molar ratio = 1.1.

that it possesses two glass transition temperatures, T_g's, which is indicative of microphase separation.[29] The lower T_g at 21 °C corresponds to the hydrophilic PDMAEMA-rich phase, while the upper T_g at 45 °C is ascribed to the fluorocarbon-rich microdomains. On the basis of these findings, the PDMAEMA-*b*-PFOMA copolymers have been annealed at 100 °C (above the upper T_g) for 24 h to provide sufficient thermal energy and time for chains to reorganize as they seek to attain thermodynamic equilibrium.[26] The (CF_3 + CF_2)/(total carbon) ratios for the annealed PDMAEMA-*b*-PFOMA samples are noticeably larger than those of the unannealed samples at all angles, indicating that annealing enhances the segregation of the PFOMA blocks to the polymer−air interface. This effect is the most pronounced for the diblock copolymer with 69 mol % PDMAEMA and may be attributed to the shorter (more mobile) PFOMA blocks present within this copolymer (see Table 2).

Since these block copolymers have been prepared as candidate membrane materials for water treatment applications, ADXPS is also used to examine the surfaces of water-exposed samples, which were first annealed at 100 °C, subsequently exposed to water for 4 h, and then vacuum-dried. Some level of reorganization of the hydrophilic PDMAEMA blocks and the low surface energy PFOMA blocks occurs upon exposure to water, as evidenced by the generally lower (CF_3 + CF_2)/(total carbon) ratios for exposed samples relative to those for the annealed samples listed in Table 4. In the case of the PDMAEMA-*b*-PFOMA copolymer with 69 mol % PDMAEMA (PDMAEMA/PFOMA molar ratio = 2.2), the ratios for annealed and water-exposed samples at 20° are identical within experimental error, implying that the surface composition remains unchanged. The accompanying ratios for water-exposed samples at 40 and 70° are lower and higher, respectively, than those corresponding to the unexposed, but annealed, samples. Since the PDMAEMA block is water-soluble, it is anticipated to migrate to the polymer−air interface in the presence of water. However, the much lower surface energy of PFOMA relative to PDMAEMA prevents the immediate surface regions from being affected. The reduction in the (CF_3 + CF_2)/(total carbon) ratio for water-exposed samples at 40° is most likely due to the migration of PDMAEMA blocks closer to the surface, while the increased ratio at 70° may reflect the displacement of PFOMA blocks to lower sampling depths. In the case of the PDMAEMA-*b*-PFOMA copolymer with 52 mol % PDMAEMA (PDMAEMA/PFOMA molar ratio = 1.1), the water-exposed samples consistently have lower (CF_3 + CF_2)/(total carbon) ratios than their unexposed analogues. These results imply that the PDMAEMA blocks migrate toward the polymer−air interface at all sampling depths.

The difference in the surface restructuring of these two block copolymers upon exposure to water is assigned to two factors: the molar concentration of PDMAEMA and the absolute size of the PFOMA block. Both copolymers have been synthesized using the same PDMAEMA-BDC macroiniferter (see Table 1) and therefore contain the same size PDMAEMA blocks ($\bar{M}_n$ = 29 000). Table 2 shows, however, that the $\bar{M}_n$ of the PFOMA block in the PDMAEMA-*b*-PFOMA copolymer with 69 mol % PDMAEMA is approximately 40 000, which is about half the size of the PFOMA block in the other diblock copolymer with 52 mol % PDMAEMA. The greater similarity in the PDMAEMA and PFOMA block sizes in the copolymer possessing 69 mol % PDMAEMA may impede PDMAEMA migration to the uppermost surface layers due to competition with PFOMA. Conversely, the hydrophilic block in the copolymer with 52 mol % PDMAEMA is much smaller relative to the PFOMA block. This size effect may permit the PDMAEMA block to migrate more easily to the polymer−air interface upon exposure to water. In this vein, another consideration is that the two copolymers with different compositions possess two different morphologies. In the copolymer with 69 mol % PDMAEMA, the similarity in block lengths may result in the formation of a layered (lamellar) morphology, whereas the copolymer with 52 mol % PDMAEMA (and longer PFOMA blocks) may form a dispersed (e.g., cylindrical) morphology. Substantial differences in morphology are expected to affect the water-induced mobility and surface migration of the blocks comprising the microdomains of the copolymers. We return to this point later.

No attempt is made to determine quantitatively the absolute surface compositions of the block copolymers for two reasons. First, the only carbon peak unique to PDMAEMA (286.8 eV) is not sufficiently well resolved, and small differences in peak areas generate large errors in calculating the surface hydrophilic concentration of each copolymer. Branching effects also preclude using the peak unique to PFOMA at 287.6 eV to determine the concentration of PFOMA. The PFOMA homopolymer possesses a branched side chain structure with ca. 22% chain branching (i.e., approximately one out of every five branches contains a fluorinated methyl branch).[24] To complement the ADXPS surface characterization and glean additional insight into surface composition, static water contact angles have been measured for PFOMA and two PDMAEMA-*b*-PFOMA copolymers. These data have been obtained by the

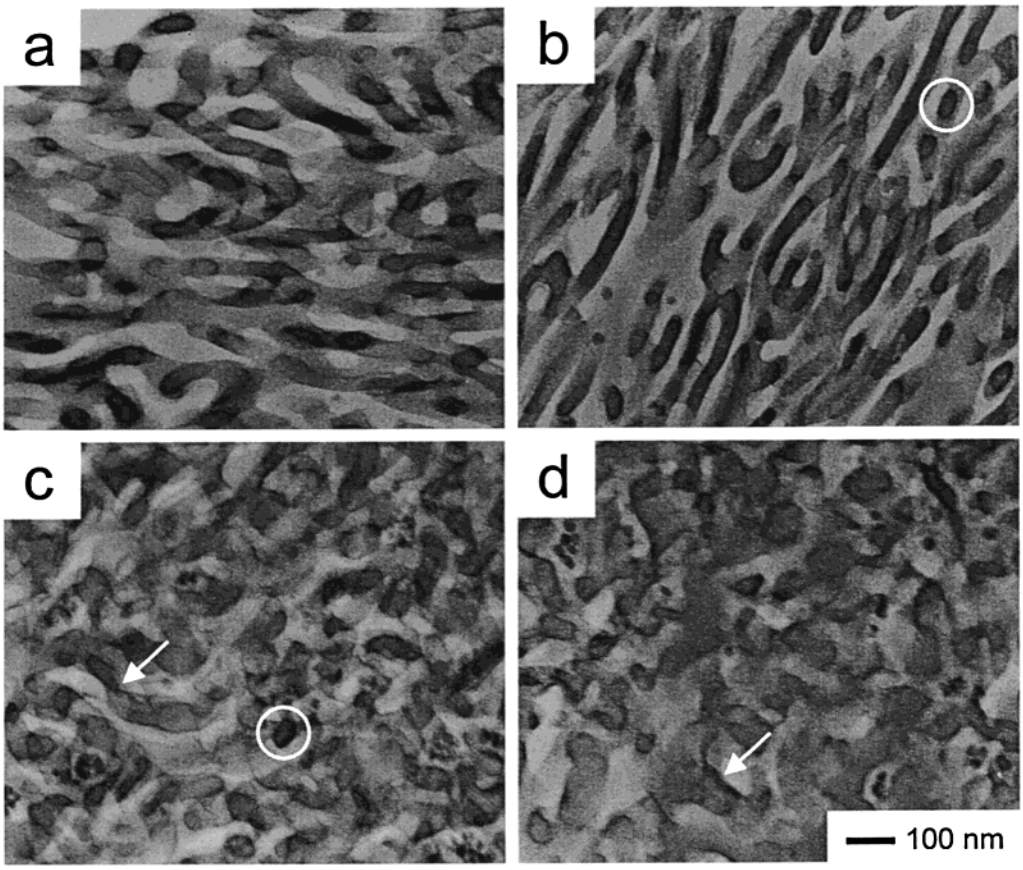

Figure 3. Transmission electron micrographs of two PDMAEMA-*b*-PFOMA diblock copolymers differing in PDMAEMA content (mol %): 55 (a, b) and 67 (c, d). These images have been collected before (a, c) and after (b, d) exposure of the copolymers to water. The hydrophilic PDMAEMA microdomains appear dark due to selective staining. The circles identify structural elements that resemble cylindrical channels, whereas the arrows locate layerlike features.

pendant drop technique from films prepared on aluminum substrates. The measured water contact angles for copolymers with 55 and 61 mol % PDMAEMA are 116 and 113 ± 1°, respectively, which are almost identical to that of the PFOMA homopolymer (117 ± 3°). Such similarity supports our assessment from ADXPS that the copolymer surfaces consist primarily of PFOMA.

Morphological Characterization of Block Copolymers. Transmission electron micrographs of PDMAEMA-*b*-PFOMA, PFOMA-*b*-PDMAEMA-*b*-PFOMA and PTAN-*b*-PDMAEMA-*b*-PTAN copolymers are displayed in Figures 3−5. In these images, the hydrophilic PDMAEMA microdomains appear electron-opaque (dark) due to selective RuO_4 staining. All of these block copolymers exhibit reasonably well-delineated, microphase-separated structural elements, regardless of previous exposure to water. The intrinsic morphology of the PDMAEMA-*b*-PFOMA diblock copolymer with 55 mol % PDMAEMA shown in Figure 3a consists of PDMAEMA cylinders residing in a PFOMA-rich matrix. In numerous instances, the cylinders (or channels) appear to be connected, forming a more complex branched morphology. No long-range order is, however, discernible. Note that this morphology differs substantially from the diblock copolymer with 67 mol % PDMAEMA in Figure 3c. This morphology is more reminiscent of a highly defective layered morphology with limited evidence of cylindrical channels and appears surprisingly similar to bicontinuous sponge morphologies observed in copolymer/solvent,[30,31] copolymer/homopolymer,[32,33] and copolymer/homopolymer/ homopolymer[34] blends. It is, however, unlike any of the morphologies presently established for neat microphase-separated block copolymers. Images of the PFOMA-*b*-PDMAEMA-*b*-PFOMA (59 mol % PDMAEMA) and PTAN-*b*-PDMAEMA-*b*-PTAN (69 mol % PDMAEMA) triblock copolymers reveal the existence of more classical morphologies, such as hexagonally packed PDMAEMA cylinders and co-alternating lamellae, in Figures 4a and 5a, respectively.

Since this family of copolymers is designed for potential use as membrane materials for water purification, it is desirable to assess the sensitivity of the copolymer morphologies to water. As is evident from the images provided in Figure 3, no obvious visual differences in morphology exist between the unexposed and water-exposed PDMAEMA-*b*-PFOMA diblock copolymers investigated in this study. Close examination of the triblock copolymers in Figures 4 and 5, however, reveals a slight, but discernible, change in the appearance of the PDMAEMA microdomains. In the case of the PFOMA-*b*-PDMAEMA-*b*-PFOMA copolymer (Figure 4), exposure to water causes the PDMAEMA cylinders to become less sharply delineated and more randomly oriented. The cylinders also appear less contiguous and resemble the structural elements generated in triblock copolymer mesogels[35−37] and mesoblends,[38] both of which incorporate a midblock-selective additive (solvent or homopolymer) into an ordered copolymer matrix by diffusion from a midblock-selective solvent. Such similarity is reasonable, since water diffuses into and alters the molecular arrangement of only the hydrophilic PDMAEMA microdomains. The PTAN-*b*-PDMAEMA-*b*-PTAN copolymer (Figure 5), on the other hand,

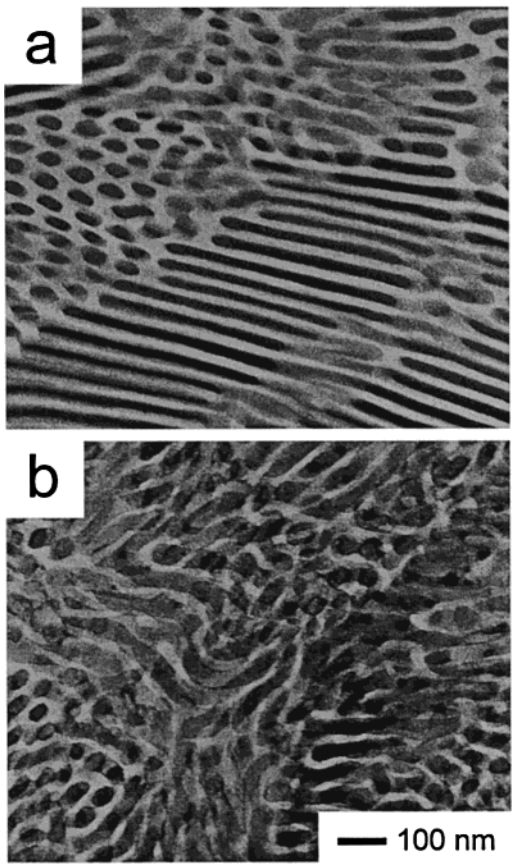

Figure 4. Transmission electron micrographs of the PFOMA-*b*-PDMAEMA-*b*-PFOMA triblock copolymer with 59 mol % PDMAEMA (a) before and (b) after exposure to water. An ordered arrangement of PDMAEMA cylinders is evident in part a, while the cylinders become more disordered and less distinct in part b.

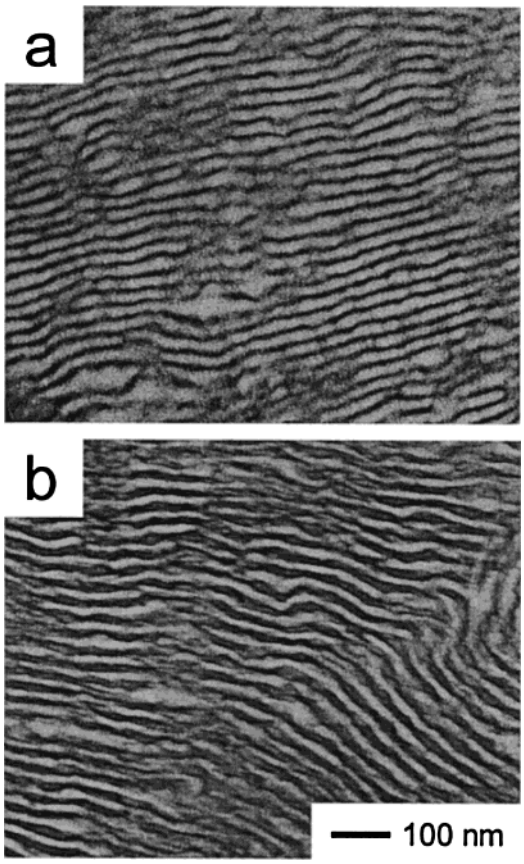

Figure 5. Transmission electron micrographs of the PTAN-*b*-PDMAEMA-*b*-PTAN triblock copolymer with 69 mol % PDMAEMA: (a) before and (b) after exposure to water. An ordered lamellar morphology is observed in both images. Exposure to water appears to induce swelling of the PDMAEMA lamellae in part b.

undergoes nonuniform swelling upon exposure to water and likewise bears close resemblance to the mesogels and mesoblends alluded to above.

To quantify the degree of morphological rearrangement, we have measured the characteristic size of the microdomains (i.e., cylindrical diameters and lamellar thicknesses) before and after exposure to water. These results are summarized for all block copolymers in Table 5. The diameters of the PDMAEMA cylinders in the PDMAEMA-*b*-PFOMA diblock copolymers are all ca. 40 nm, which is consistent with the relatively invariant size of the PDMAEMA blocks (27 000−32 000). These dimensions do not, within experimental uncertainty, change upon exposure to water. Similarly, the diameter of the hydrophilic PDMAEMA microdomains in the PFOMA-*b*-PDMAEMA-*b*-PFOMA triblock copolymer remains constant at ca. 25 nm. In contrast, the PDMAEMA lamellae in the PTAN-*b*-PDMAEMA-*b*-PTAN triblock copolymer increase measurably upon exposure to water. The PTAN lamellae, on the other hand, are not as strongly influenced by water, decreasing from 12.1 ± 0.9 nm (unexposed) to 10.0 ± 1.6 nm (exposed). The difference in the response of the two triblock copolymers to water may be attributed to the inherent difference in their morphologies (cylindrical vs lamellar) and the ability of PTAN to crystallize.[17,24,39] The latter consideration is expected to assist in ordering the PTAN lamellae. In summary, there appears to be little, if any, morphological rearrangement of the PFOMA-containing diblock and triblock copolymers in the presence of water. The PTAN-*b*-PDMAEMA-*b*-PTAN triblock copolymer, however, shows limited evidence of water-induced lamellar swelling.

Table 5. Morphological Characteristics of Several Block Copolymers

copolymer (mol % PDMAEMA)	morphology	PDMAEMA microdomain size (nm)	
		unexposed	exposed
	PDMAEMA-*b*-PFOMA		
55	cylindrical	37.3 ± 0.6	39.0 ± 2.3
67	cylindrical/ layered	37.2 ± 5.8	38.4 ± 2.4
	PFOMA-*b*-PDMAEMA-*b*-PFOMA		
59	cylindrical	25.0 ± 3.3	25.0 ± 1.5
	PTAN-*b*-PDMAEMA-*b*-PTAN		
69	lamellar	11.5 ± 1.0	17.4 ± 3.2

Water Uptake and Water Flux. Water uptake is shown as a function of PDMAEMA concentration in Figure 6. The PFOMA and PTAN blocks are highly hydrophobic (they only sorb 1−2 wt % water),[17] while PDMAEMA is water-soluble. Hence, it is not surprising that water uptake increases with increasing PDMAEMA content in the series of diblock copolymers. Interestingly, the PFOMA-*b*-PDMAEMA-*b*-PFOMA and PTAN-*b*-PDMAEMA-*b*-PTAN triblock copolymers sorb approximately 50% less and 40% more water, respectively, than the PDMAEMA-*b*-PFOMA diblock copolymers with similar hydrophilic content. This result is attributed to differences in water accessibility of the hydrophilic microdomains in the microphase-separated

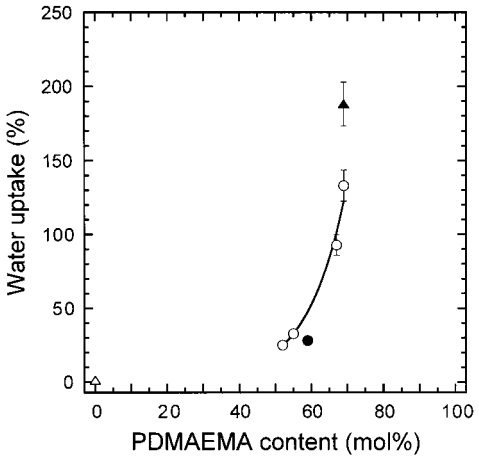

Figure 6. Composition dependence of water uptake in PFOMA/PTAN homopolymers (△), PDMAEMA-*b*-PFOMA diblock copolymers (○), a PFOMA-*b*-PDMAEMA-*b*-PFOMA triblock copolymer (●), and a PTAN-*b*-PDMAEMA-*b*-PTAN (▲) triblock copolymer at 25 °C.

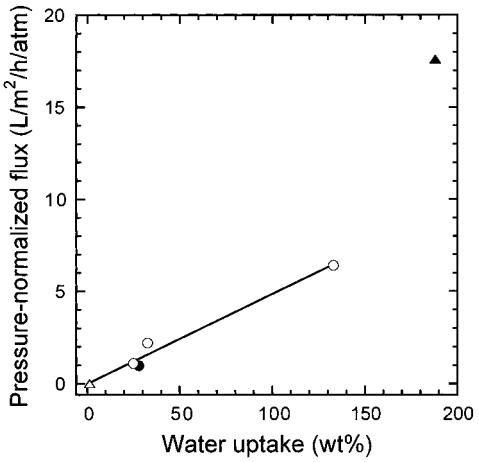

Figure 7. Dependence of pressure- and thickness-normalized water flux on water uptake in PFOMA/PTAN hompopolymers (△), as well as in the PDMAEMA-*b*-PFOMA (○), PFOMA-*b*-PDMAEMA-*b*-PFOMA (●), and PTAN-*b*-PDMAEMA-*b*-PTAN (▲) copolymers at 25 °C.

block copolymers, which possess different architectures, morphologies and crystallizability. The high water uptake of the PTAN-*b*-PDMAEMA-*b*-PTAN copolymer is entirely consistent with its lamellar morphology (see Figure 5), which ensures access of water molecules to the PDMAEMA moieties. Moreover, the microdomain thickness data provided in Table 5 indicate that the PDMAEMA microdomains in this triblock copolymer are the only ones to swell measurably upon exposure to water, confirming that these hydrophilic regions are more accessible to water than those in the other copolymers.

Figure 7 presents the pressure-normalized flux as a function of water uptake. These values are also normalized to a film thickness of 1 μm, so that the permeation properties of different block copolymers, as well as other membrane materials, can be compared in a meaningful fashion. In general, water flux increases with increasing water uptake and, in turn, with hydrophilic PDMAEMA content. This correlation indicates that water uptake measurements can be employed as a valuable screening tool in the design of novel membrane materials. The pressure-normalized flux value for the PFOMA-*b*-PDMAEMA-*b*-PFOMA triblock copolymer is comparable to those of the PDMAEMA-*b*-PFOMA diblock copolymers with similar hydrophilic content. Recall from Figures 3 and 4 that these copolymers all exhibit dispersed morphologies that consist of PDMAEMA cylinders in a continuous matrix. The PDMAEMA cylinders in the PFOMA-*b*-PDMAEMA-*b*-PFOMA triblock copolymer measure about 25 nm in diameter and are substantially smaller and more highly ordered than those of the corresponding diblock analogues. This result suggests that the continuity of the hydrophilic microdomains throughout the membrane and their accessibility to water are more important than the actual size of the microdomains.

The water uptake of the PDMAEMA-*b*-PFOMA copolymer with 69 mol % PDMAEMA is much higher (about 135 wt %) than that of the diblock copolymers with lower PDMAEMA content (between 25 and 100 wt %, depending on composition). This copolymer also has a higher water flux than the other PDMAEMA-*b*-PFOMA diblock copolymers or the PFOMA-*b*-PDMAEMA-*b*-PFOMA triblock copolymer, strongly suggesting that the PDMAEMA microdomains in this copolymer are more continuous than those in the other PFOMA-containing block copolymers. This implication is substantiated by its morphology (see Figure 3), which we have classified as a complex combination of disordered cylinders and layers (see Table 5). The PTAN-*b*-PDMAEMA-*b*-PTAN triblock copolymer exhibits the highest water flux of all the copolymers investigated in this study. This observation, which is consistent with the ability of this copolymer to sorb the most water, strongly supports our contention that the PDMAEMA lamellae are continuous throughout the thickness of the film.

Interestingly, water permeation occurs through the PDMAEMA-*b*-PFOMA diblock copolymers with 52 and 69 mol % PDMAEMA even though ADXPS shows that the $(CF_3 + CF_2)$/(total carbon) ratios at the polymer−air interface are very similar to that of the PFOMA homopolymer. In marked contrast, no measurable water permeation is observed over a period of 24 h for a PFOMA homopolymer film. These results corroborate our earlier conclusion that some of the PDMAEMA microdomains reside at the polymer−water interface and are accessible to water transport. Several possible explanations may account for this scenario. First, however, the limitations of ADXPS and TEM used to probe the surface and morphological characteristics of the block copolymers examined here must be recognized. Neither technique can be used in situ, i.e., while the polymer is subjected to an aqueous environment. Furthermore, the samples are vacuum-dried prior to analysis to avoid problems with the cryoultramicrotome and the spectrometer. Thus, we must assume that the copolymer characteristics determined ex situ are representative of those in the presence of water. Complementary analytical techniques capable of probing hydrated surface and bulk morphologies are needed to describe more accurately the effect of water on the surface morphology of these copolymer membranes. With this limitation notwithstanding, however, we now turn our attention to the environmental responsiveness of microphase-separated block copolymers.

It is well-established that block copolymers can respond sensitively to their environment. Miyata et al.,[15] for example, report differences between the features of the air- and glass-side surfaces of poly(methyl meth-

acrylate)-*b*-poly(dimethylsiloxane) (PMMA-*b*-PDMS) block copolymer membranes. As the surface becomes more hydrophobic, more of the PDMS chains migrate to the polymer−air interface to minimize the surface free energy. Exposure of microphase-separated diblock copolymers to a permeant with a high degree of affinity for one or both blocks may, at sufficiently high sorption levels, promote a morphological transition under isothermal conditions.[40,41] Since PDMAEMA is water-soluble, rearrangement of the PFOMA and PDMAEMA chains at the polymer−water interface is expected to promote changes in surface properties and morphology. Recall that the water-exposed PDMAEMA-*b*-PFOMA copolymer with 52 mol % PDMAEMA possesses slightly lower values of the $(CF_3 + CF_2)$/(total carbon) ratio at all sampling angles than its annealed analogues, implying that some PDMAEMA chains migrate to the polymer−air interface. Differences in the ratios for the water-exposed and annealed diblock copolymer with 69 mol % PDMAEMA provide further evidence for water-induced chain rearrangement. Regardless of whether more pronounced rearrangement of the PFOMA and PDMAEMA chains occurs during testing, the water uptake and water flux values reported in the present work clearly reveal that some of the hydrophilic domains not only are accessible to the surfaces of the copolymer films but also wind continuously throughout the thickness of the films.

Conclusions

Block copolymers composed of a very low surface energy (<11 dyn/cm)[27,28] fluorocarbon block (PFOMA or PTAN) and a hydrophilic block (PDMAEMA) have been synthesized by a two-component iniferter technique. Monofunctional or bifunctional telechelic PDMAEMA is first produced as the iniferter. Diblock copolymers are prepared by the subsequent polymerization of the fluorocarbon monomer. Since molecular weight determination of telechelic PDMAEMA is problematic, the molecular weights are provided on the basis of a perfect living polymerization. The hydrophilic PDMAEMA content of the block copolymers is, however, obtained directly from ^{1}H NMR. Surface and morphological characterization of these materials indicates that they are microphase-separated under the conditions explored in this study. According to ADXPS, the surfaces of the PDMAEMA-*b*-PFOMA films are chemically similar to that of PFOMA, implying that the low surface energy fluorinated blocks segregate to the polymer−air interface. Static water contact angles measured from two diblock copolymers are also comparable to that of PFOMA, thereby supporting the ADXPS results. Upon exposure to water, the polymer chains at the surface rearrange to minimize the free energy, as evidenced by measurable changes in the ADXPS spectra. Transmission electron micrographs of the copolymers confirm that these materials are all microphase-separated. The PDMAEMA-*b*-PFOMA diblock copolymers exhibit either disordered (possibly defect-ridden) cylindrical and/or layered morphologies, depending on composition. The PFOMA-*b*-PDMAEMA-*b*-PFOMA triblock copolymer possesses a reasonably well-ordered cylindrical morphology, while the PTAN-*b*-PDMAEMA-*b*-PTAN molecules microphase-separate into lamellar microdomains. As anticipated, water uptake increases with increasing copolymer hydrophilicity (PDMAEMA content). Water flux also increases with increasing water uptake, indicating that water uptake measurements constitute a valuable screening technique in the development of novel membrane materials for water purification. Since water flux cannot be correlated with the characteristic size of the hydrophilic microdomains, we conclude that the accessibility of the PDMAEMA-rich regions, as well as the morphology and crystallizability of the copolymers, influence water permeation behavior.

Acknowledgment. This work was supported in part by the Office of Naval Research, the National Water Research Institute, the National Science Foundation (Presidential Faculty Fellowship, J.M.D., 1993−1997), the American Water Works Association Research Foundation, the STC program of the National Science Foundation under Agreement No. CHE9876674, and the Strategic Environmental Research and Defense Program.

References and Notes

(1) Riley, R. L. In *Membrane Separation Systems: Recent Developments and Future Directions*; Baker, R. W., Cussler, E. L., Eykamp, W., Koros, W. J., Riley, R. L., Strathmann, H., Eds.; Noyes Data Corporation: Park Ridge, NJ, 1991; Vol. 2, p 276.
(2) Mallevialle, J.; Odendaal, P. E.; Wiesner, M. R. *Water Treatment Membrane Processes*; McGraw-Hill: New York, 1996.
(3) Baker, R. W. *Membrane Technology and Applications*; McGraw-Hill: New York, 2000.
(4) Baker, R. In *Membrane Technology in the Chemistry Industry*; Nunes, S. P., Peinemann, K.-V., Eds.; Wiley-VCH: Weinheim, Germany, 2001; p 268.
(5) Hamza, A.; Pham, V. A.; Matsuura, T.; Santerre, J. P. *J. Membr. Sci.* **1997**, *131*, 217.
(6) Spontak, R. J.; Alexandridis, P. *Curr. Opin. Colloid Interface Sci.* **1999**, *4*, 140.
(7) Bates, F. S.; Fredrickson, G. H. *Phys. Today* **1999**, *52*, 32.
(8) Otsu, T.; Kuriyama, A. *Polym. Bull. (Berlin)* **1984**, *11*, 135.
(9) Otsu, T.; Kuriyama, A. *Polym. J.* **1985**, *17*, 97.
(10) Otsu, T.; Matsumoto, A. *Adv. Polym. Sci.* **1998**, *136*, 75.
(11) Otsu, T. *J. Polym. Sci., Part A: Polym. Chem.* **2000**, *38*, 2121.
(12) Choi, Y.-K.; Lee, S.-B.; Lee, D.-J.; Ishigama, Y.; Kajiuchi, T. *J. Membr. Sci.* **1998**, *148*, 185.
(13) Dutta, B. K.; Sidkar, S. K. *Environ. Sci. Technol.* **1999**, *33*, 1709.
(14) Knoell, T.; Safarik, J.; Cormack, T.; Riley, R.; Lin, S. W.; Ridgway, H. *J. Membr. Sci.* **1999**, *157*, 117.
(15) Miyata, T.; Obata, S.; Uragami, T. *Macromolecules* **1999**, *32*, 8465.
(16) Miyata, T.; Obata, S.; Uragami, T. *J. Polym. Sci., Part B: Polym. Phys.* **2000**, *38*, 584.
(17) Nagai, K.; Tanaka, S.; Hirata, Y.; Nakagawa, T.; Arnold, M. E.; Freeman, B. D.; Leroux, D.; Betts, D. E.; DeSimone, J. M.; DiGiano, F. A. *Polymer* **2001**, *42*, 9941.
(18) Miyata, T.; Obata, S.; Uragami, T. *Macromolecules* **1999**, *32*, 3712.
(19) Guan, Z.; DeSimone, J. M. *Macromolecules* **1994**, *27*, 5527.
(20) Doi, T.; Matsumoto, A.; Otsu, T. *J. Polym. Sci., Part A: Polym. Chem.* **1994**, *32*, 2911.
(21) Seah, M. P.; Dench, W. A. *Surf. Interface Anal.* **1979**, *1*, 2.
(22) Chen, X.; Lee, H. F.; Gardella, J. A. *Macromolecules* **1993**, *26*, 4601.
(23) Betts, D. E. Ph.D. Dissertation, The University of North Carolina at Chapel Hill, 1998.
(24) Kassis, C. M.; Steehler, J. K.; Betts, D. E.; Guan, Z.; Romack, T. J.; DeSimone, J. M.; Linton, R. W. *Macromolecules* **1996**, *29*, 3247.
(25) Beamson, G.; Briggs, D. *High-Resolution XPS of Organic Polymers: The Scienta ESCA300 Database*; John Wiley & Sons: New York, 1992.
(26) Kassis, C. M. Ph.D. Dissertation, The University of North Carolina at Chapel Hill, 1997.
(27) Pittman, A. G. In *Fluoropolymers*; Wall, L. A., Ed.; John Wiley & Sons: New York, 1972; p 419.
(28) Ramharack, R.; Nguyen, T. H. *J. Polym. Sci., Polym. Lett. Ed.* **1987**, *25*, 93.
(29) Utracki, L. A. *Polymer Alloys and Blends*; Hanser: Berlin, 1990.

(30) Hecht, E.; Mortensen, K.; Hoffmann, H. *Macromolecules* **1995**, *28*, 5465.
(31) Förster, S.; Berton, B.; Hentze, H.-P.; Krämer, E.; Antonietti, M.; Lindner, P. *Macromolecules* **2001**, *34*, 4610.
(32) Laurer, J. H.; Fung, J. C.; Sedat, J. W.; Smith, S. D.; Samseth, J.; Mortensen, K.; Agard, D. A.; Spontak, R. J. *Langmuir* **1997**, *13*, 2177.
(33) Bates, F. S.; Maurer, W. W.; Lipic, P. M.; Hillmyer, M. A.; Almdal, K.; Mortensen, K.; Fredrickson, G. H.; Lodge, T. P. *Phys. Rev. Lett.* **1997**, *79*, 849.
(34) Laurer, J. H.; Smith, S. D.; Samseth, J.; Mortensen, K.; Spontak, R. J. *Macromolecules* **1998**, *31*, 4975.
(35) Folkes, M. J.; Keller, A. *J. Polym. Sci., Part B: Polym. Phys. Ed.* **1976**, *14*, 833.
(36) Folkes, M. J.; Keller, A.; Odell, J. A. *J. Polym. Sci., Part B: Polym. Phys.* **1976**, *14*, 847.
(37) King, M. R.; White, S. A.; Smith, S. D.; Spontak, R. J. *Langmuir* **1999**, *15*, 7886.
(38) Roberge, R. L.; Patel, N. P.; White, S. A.; Thongruang, W.; Smith, S. D.; Spontak, R. J. *Macromolecules* **2002**, *35*, 2268.
(39) *Organofluorine Chemistry: Principles and Commercial Applications;* Banks, R. E., Smart, B. E., Tatlow, J. C., Eds.; Plenum Press: New York, 1994.
(40) Hong, S.-U.; Laurer, J. H.; Zielinski, J. M.; Samseth, J.; Smith, S. D.; Duda, J. L.; Spontak, R. J. *Macromolecules* **1998**, *31*, 2174.
(41) Zielinski, J. M. In *Encyclopedia of Materials: Science and Technology*; Buschow, K. H. J., Cahn, R. W., Flemings, M. C., Ilschner, B., Kramer, E. J., Mahajan, S., Eds.; Elsevier: Oxford, England, 2001; Vol. 1, p 739.

MA0119631